

Article

Sustainable Applications of Tyre-Derived Aggregates for Railway Transportation Infrastructure

Mohammad Adnan Farooq , Sanjay Nimbalkar *  and Behzad Fatahi

School of Civil and Environmental Engineering, University of Technology Sydney, Ultimo, NSW 2007, Australia

* Correspondence: Sanjay.Nimbalkar@uts.edu.au

Abstract: Scrap tyres are used to produce tyre-derived aggregates (TDA), which can be used as fill material, backfill material, drainage layers, and vibration-damping material, among other uses. This study presents a comprehensive review of TDA applications in civil engineering with a specific focus on railway projects. A review of the existing literature reveals the lack of sufficient knowledge on the use of TDA in slab tracks. This article also analyses the adequacy of different constitutive models to properly simulate the performance of TDA while highlighting the importance of adopting the most suitable constitutive model. The variations in shear stresses and displacements with depth below ballasted and slab tracks in the presence and absence of TDA are discussed. It is shown that TDA effectively reduces the shear stresses for the subgrade layer of both track types. Moreover, the impact of TDA on stress transfer in the vertical and lateral track directions is assessed. The findings from the present analysis reveal that TDA helps in reducing the vertical and lateral stresses near its placement position in ballasted and slab tracks.

Keywords: tyre-derived aggregates; finite element modelling; railway track; scrap tyre; shear stress



Citation: Farooq, M.A.; Nimbalkar, S.; Fatahi, B. Sustainable Applications of Tyre-Derived Aggregates for Railway Transportation Infrastructure. *Sustainability* **2022**, *14*, 11715. <https://doi.org/10.3390/su141811715>

Academic Editors: Marc A. Rosen and Fernanda Bessa Ferreira

Received: 13 July 2022

Accepted: 15 September 2022

Published: 18 September 2022

Publisher's Note: MDPI stays neutral with regard to jurisdictional claims in published maps and institutional affiliations.



Copyright: © 2022 by the authors. Licensee MDPI, Basel, Switzerland. This article is an open access article distributed under the terms and conditions of the Creative Commons Attribution (CC BY) license (<https://creativecommons.org/licenses/by/4.0/>).

1. Introduction

Different waste materials have been researched for their applications as construction materials in past decades. For example, demolition waste [1], steel furnace slag [2], recycled glass [3], fly ash [4], and scrap tyres [5–7] have been assessed for their suitability as railway track material. In particular, rubber has a profound influence on the environment and comes in different forms and at the end of its life, it becomes waste. Rubber is used in our daily routine, viz., protection gloves, tubes, mattresses, and tyres. All these are significant sources of rubber waste. Rubber waste can be recycled, re-used or both. Gloves and mattresses can only be recycled, while tyres and tubes can either be recycled or re-used [8].

Each year, approximately 70 million tons of scrap tyres is produced globally, of which 52% and 14% are disposed of through burning and landfilling, respectively [9]. The amounts of 16% and 12% of the discarded tyres are utilised to produce bitumen/concrete and rubber, respectively [9,10]. The amount of scrap tyres is increasing worldwide with an annual production of 12.6, 6.4, and 8 kg/resident in the USA, Europe, and Japan, respectively [11]. In Australia alone, over 50 million tyres are discarded yearly [12].

In the USA, more than half of scrap tyres are converted into tyre-derived fuel, 24.4% are used to produce ground rubber, 8.2% are disposed in landfills, and 4.3% are used for civil engineering applications [13]. Landfilling waste tyres require a large amount of space due to their incompressible nature. Shredding tyres is an alternative, but high operational costs render this option rather unfeasible. In Japan, the vast majority of scrap tyres are recycled as fuel, resulting in excessive carbon dioxide and incineration ash generation [14]. The burning of these scrap tyres also contributes to the temperature rise in that region, and the resulting residue pollutes the soil. The annual disposal of scrap tires is estimated to reach 400% by 2030 [13]. Recycling waste rubber helps reduce large amounts of energy, eventually reducing greenhouse gas emissions. It has been estimated that recycling four

tyres reduces CO₂ emissions by approximately 146 kg, equivalent to 69 litres of gasoline. In addition to environmental benefits, scrap rubber recycling plays a significant role in powering up the economy and creating jobs. More than USD 1.6 billion in the United States was generated as revenue in the rubber recycling industry [15]. Hence, it has become prudent to investigate scrap tyres as a prospective geomaterial for various civil engineering applications.

This paper has been divided into two parts. In the first part, an introduction to scrap tyres is provided, including their civil engineering applications, shear strength, and compressibility properties. Indeed, the use of scrap rubber in ballasted tracks has been a topic of interest in recent times. On the contrary, very limited knowledge is available on its use in slab tracks. The second part of this paper deals with the finite element simulation of ballasted and slab tracks including and excluding TDA. Previous studies [16,17] have modelled TDA as an elastic material and very limited studies [5,18] have considered TDA as a hyperelastic material. The present study discusses the stress–strain response of TDA considering different hyperelastic models and attempts to identify the most suitable hyperelastic strain energy potential. As per the authors' knowledge, for the first time, the variations in the different components of shear stress and displacement with depth for ballasted and slab tracks, without and with TDA, is presented. The study also shows the effects of train speed and axle load on the vertical and lateral stress distribution of ballasted and slab tracks while incorporating TDA.

2. Scrap Tyres

According to ASTM D 6270, "Standard practice for the use of scrap tyres in civil engineering applications", a scrap tyre is defined as a damaged tyre and which can be processed again for its originally intended use or some other applications [19]. However, scrap tyres are a significant source of pollution; these scrap tyres consist of natural and synthetic rubber elastomers derived during the fractional distillation of crude oil. In addition, various polymers, metals, and additives are added during the production of tyres to improve their resistance to harsh environmental conditions. Hence, they can be regarded as inert materials due to their prolonged decomposition time [20]. This characteristic of scrap tyres justifies their widespread application in civil engineering projects. These scrap tyres can be used to produce tyre-derived aggregates (TDA) for potential use in various construction projects. The recycled materials obtained from waste tyres can be classified into tyre shreds (50–305 mm), tyre chips (12–50 mm), granulated rubber (<12 mm), ground rubber (<2 mm), and powdered rubber (<0.425 mm) [19,21]. TDA is a mixture of tyre shreds (50–305 mm) and tyre chips (12–50 mm) [22,23].

2.1. Advantages of Using Scrap Tyres

Recycling scrap tyres can be challenging due to their large size, but it is worth the additional effort. The primary benefits associated with rubber recycling include a lower consumption of energy, less pressure on natural rubber, the conservation of landfill space, a reduction in environmental pollution, and the creation of new products [24]. Figure 1 shows the life cycle of tyres and civil engineering applications of scrap tyres. Four key advantages of recycling scrap tyres can be summarized as below:

- Conservation of landfill space: Tyres occupy ample space in landfills [25]. Landfill space is limited and expensive; hence, using scrap types helps save this space for things which are difficult to recycle [26].
- Creation of beneficial products: Recycled tyres can be converted into a plethora of valuable products, viz., tyre-derived fuel [8], rubberised asphalt [27], flooring [28], railway sleepers [29], and playground turf [26].
- Prevention of the spread of diseases: Discarded scrap tyres serve as a habitat for the growth of disease-carrying rodents. Moreover, stagnant water gets collected inside them, which serves as a breeding ground for flies [26,30].

- Prevention of fires and pollution: One of the significant disadvantages associated with stockpiling scrap tyres is fire hazard. For example, a fire broke out in Melbourne in 2016, and more than 150,000 tyres were burnt, which led to the release of harmful gases into the environment [31]. Hence, re-using these scrap tyres is highly recommended and stockpiling should be avoided.

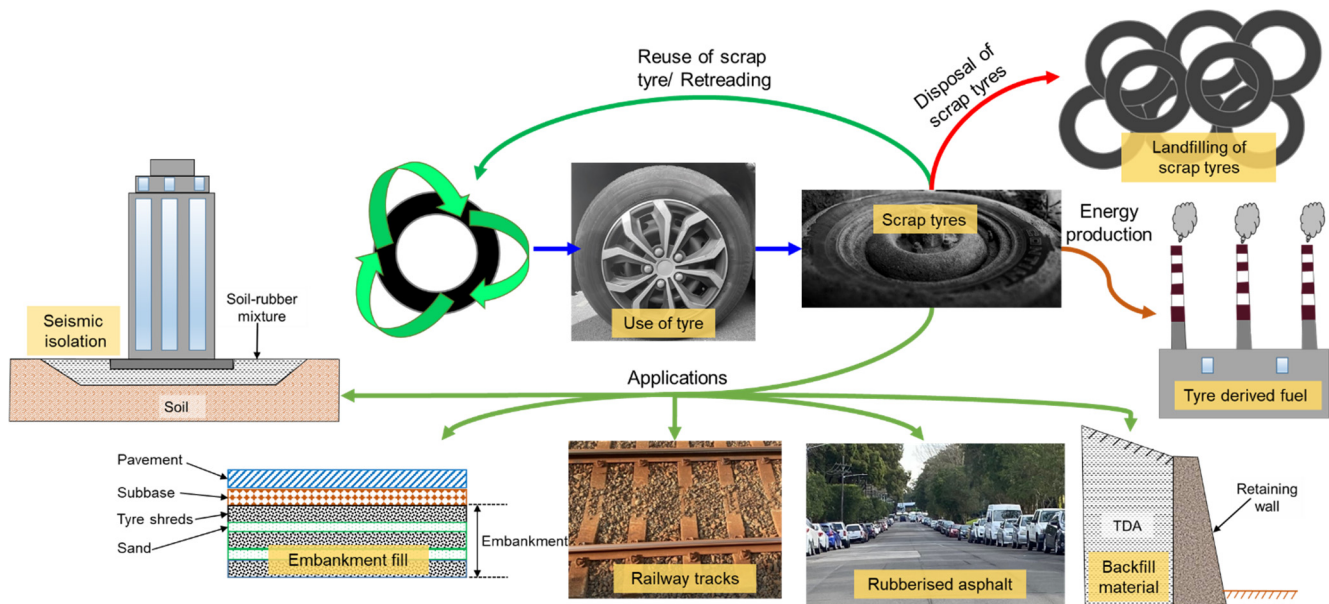


Figure 1. Life cycle and civil engineering applications of scrap tyres.

2.2. Civil Engineering Applications for Scrap Tyres

Scrap tyres are increasingly used for various civil engineering applications, as elaborated upon below:

- Embankment and trench fill material: Tyre shreds are beneficial as lightweight fill material when constructing embankments on soft soils. Low unit weight (approximately 40% compared to compacted soil) and low cost render them appropriate fill material [32–34].
- Backfill material for retaining walls and bridge abutments: The low unit weight of these materials aids in reducing the active lateral pressures acting on the backface of retaining walls, which further helps to construct thinner wall sections. The rapid drainage of these materials also helps to limit the build-up of excess hydrostatic pressure behind the walls [34–37].
- Drainage layer in highway construction: They are also used as a drainage layer for the construction of roads [38].
- Vibration damping material in railway tracks: Scrap tyres in the form of TDA have been used as damping material for better attenuation of vibration associated with the passage of a train [39,40].
- Leach drain for septic systems: Clean-cut and uniform-size scrap tyres have been used to replace conventional stone backfill material in septic sewage disposal systems [41].
- Protection cushion and isolation layer against seismic forces: Tyre shreds have been used in trench barriers as an isolation medium for vibration attenuation [23,42]. Tyre chips placed as layers or mixed with sand help in seismic isolation [19].
- Asphalt rubber: Scrap tyres are commonly used to produce asphalt rubber. Ground rubber (<2 mm) is blended with asphalt to reduce skid distance and noise and improve durability while having favourable implications for cost reduction. Some studies report their use as aggregates [43] and in asphalt mixes [44].

- Building aggregates/fillers: Waste rubber materials have been used as building aggregates or fillers and have been shown to lower the thermal conductivity of cementitious materials by up to 50% [45].
- Subgrade insulation in roads: The thawing of subgrade soil releases excess water in cold regions. To avoid this problem, tyre shreds in layers (150–300 mm) are placed below the road surface, shielding the subgrade from the cold temperatures. Scrap tyres help to protect against frost-susceptible soils [46,47].

2.3. Shear Strength and Compressibility Characteristics of Tyre Shreds

Tyre shreds are similar to coarse gravel and crushed rock in terms of gradation characteristics; however, they differ in terms of shear strength and compressibility. The shear strength and compressibility behaviour of soil-scrap rubber mixtures are elaborated below.

- Shear strength: The shear strength behaviour of sand-scrap rubber mixtures depends on the type of scrap rubber. The addition of tyre shreds or tyre chips increases the shear strength of sand [48], while the inclusion of tyre crumbs reduces the shear strength of sand [49,50].
- Compressibility: The compressibility of rubber mixtures is inversely proportional to the soil proportion [51]. The increase in the proportion of tyre crumbs increases the compressibility of the soil-rubber mixtures [50]. The size of scrap rubber (small tyre chips and larger shreds) does not influence rubber response [32].

2.4. Application of Scrap Rubber in Railway Engineering

Based on the discussion in the preceding paragraphs, the advantages of using scrap rubber in railway tracks compared to other applications include:

- The use of scrap rubber tyres as fuel releases a significant amount of CO₂ into the atmosphere and also generates a huge amount of incineration ash [14]. However, using scrap tyres on railway tracks would minimise the excessive release of CO₂ and reduce the amount of incineration ash. It would also help to reduce the global warming associated with burning these scrap tyres that contributes to the temperature rise in the region.
- Scrap tyres occupy a huge amount of landfill space [25]. Hence, using scrap tyres on railway tracks would help preserve the landfill space.
- Compared to other civil engineering applications such as embankment and backfill, scrap tyres replace expensive resilient materials, such as geosynthetics and rubber mats, used in railway tracks to attenuate noise, vibration [52], and track deformation [53,54]. Hence, it would help in reducing the construction costs of railway tracks.

Recently, scrap rubber has been used in railway engineering to attenuate environmental vibrations due to moving trains [5,55]. Esmaeili et al. [55] performed field trials using TDA as a layer below ballast. They observed that the vibration reduction efficiency of TDA was comparable to the ballast mat [55]. A finite element study by Farooq et al. [5] showed that scrap rubber (in the form of TDA) helps reduce the stress levels near the zone of TDA placement in both ballasted and slab tracks. In addition, TDA incorporation lowers the vibration levels of ballasted and slab tracks by 42% and 50%, respectively [5].

Fathali et al. [56] recommended a 10% optimum dosage for TDA, which helped reduce particle breakage and settlement by 47% and 6%, respectively [56]. Esmaeili et al. [57] evaluated the performance of TDA (0, 5, 10, and 15%) in fouled ballasted tracks using cyclic uniaxial tests and recommended a 5% dosage as optimum considering breakage and stiffness [57]. In addition, the damping ratio increased with increasing TDA proportions [57]. In another study, Song et al. [58] observed that the damping ratio increased while the resilient interface shear stiffness reduced due to the addition of TDA to the ballast. In addition, peak shear stress, dilation effect, cohesion, and friction angle of ballast were reduced due to TDA incorporation. An optimum TDA dosage of 5% was recommended [58].

Gong et al. [17] performed large-scale direct shear testing (DST) and discrete element modelling (DEM) of the ballast-TDA mixture and revealed that TDA notably reduced the

shear stress and dilation effect of the ballast-TDA mixture. DST showed that the ballast breakage index decreased by 53% with a 10% TDA addition, and DEM showed that TDA reduced the magnitude of contact forces, implying less breakage of ballast aggregates [17]. Ho et al. [59] developed a new material, resilient bound ballast (RBB), comprising ballast mixed with TDA bonded using a resilient epoxy binder. RBB showed improved strength over traditional ballast and could be used below concrete ties, leading to reduced abrasion and ballast fouling [59]. A mixture of waste rubber and polyurethane has been used as a waterproofing layer on high-speed railway tracks. It has shown excellent results compared to the traditional asphalt concrete layer [60]. One study suggested that using TDA below sleepers would help improve the lateral resistance of railway tracks [61]. Hence, it is seen that the application of scrap rubber has been investigated for ballasted tracks by many studies. In contrast, its application for slab tracks has been assessed by limited studies [5,60], as summarized in Tables 1 and 2. Hence, further research is recommended in this area.

Table 1. Summary of research findings related to TDA application in railway tracks.

Methodology	Track Type	Major Findings	Reference
Finite element modelling	Ballasted and slab tracks	The TDA reduced peak acceleration for both track types. Vertical stress reduction occurred near the zone of TDA placement in both track types.	[5]
Finite element modelling and field testing		The presence of TDA reduced bridge deck acceleration and deflection.	[55]
Discrete element modelling and laboratory testing	Ballasted track	The addition of TDA (10% by volume) reduced the stiffness of the ballast while improving the stiffness of the fouled ballast.	[61]
Field testing		TDA incorporation reduced peak shear stress, dilation, and ballast breakage.	[17]
Laboratory testing		The vibration reduction effectiveness of the TDA was comparable to or higher than that of ballast mats.	[62]
		Reduction in ballast breakage and vibrations.	[56]
		Both TDA and sand increased the settlement of railway tracks. TDA was more effective in reducing ballast breakage for fully fouled conditions.	[57]
		The addition of TDA enhanced the damping ratio while causing a loss in mechanical properties.	[58]
		The addition of TDA and epoxy enhanced cohesive strength and reduced ballast breakage.	[59]
		The application of TDA in a specified volume (1500–2000 cm ³) under the sleeper improved the lateral resistance of the track.	[63]
		Adding up to 10% TDA to slag ballast material helped to reduce grain crushing and increase the damping ratio of the mix. Although settlement increased, it was under permissible limit.	[64]

Table 2. Summary of research findings related to scrap rubber (in form of tyre, powder, granulates, shreds, and crumb) in railway tracks.

Methodology	Track Type	Scrap Rubber Type	Major Findings	Reference
Finite element modelling	Ballasted track	Rubber tyre	The tyre reinforcement provided additional confinement, which helped to reduce the vertical and lateral track deflections, especially for soft foundations.	[65]
Finite element modelling and laboratory testing	Slab track	Waste rubber powder	The proposed layer (waste rubber and thermoplastic polyurethane) showed better performance as a waterproof seal layer compared to the asphalt concrete layer.	[60]
		Granulated rubber	The newly developed material (rubber granules bonded with polyurethane) showed good performance under compression and shear loading, which makes it an excellent choice for use as an anti-vibration mat on railway tracks.	[66]
Discrete element modelling and finite difference modelling	Ballasted track	Crumb rubber	Although the accelerations of the train, rail, and sleeper increased due to the use of crumb rubber in the ballast layer, a reduction in ballast degradation, subgrade surface acceleration, and subgrade surface stress was observed.	[67]
Discrete element modelling and laboratory testing			The rubber-protected ballast provided more homogenous contact forces and better force distribution compared to ballast.	[68]
Field testing		Tyre shreds	The use of tyre shreds under ballast and sleeper is both a practical and viable solution for ground-borne vibration reduction at a significantly lower cost.	[40]
Laboratory testing		Rubber shreds	The addition of rubber shreds (up to 10%) with granular soil increased the damping ratio by up to 95%, suggesting the potential ability of the mix to attenuate vibrations.	[39]
	Granulated rubber	The shear strength and liquefaction resistance of the new subgrade filler were better than pure sand.	[69]	
		The incorporation of granulated rubber reduced the fluctuations in the sleeper–rail oscillation after the routine track maintenance process.	[70]	
		Fibres enhanced the flexural and shear performance; crumb rubber improved the flexibility of the mix.	[71]	
	Crumb rubber	The proposed rubber-coated ballast showed better performance in terms of abrasion, breakage, and long-term settlement.	[72]	
		The smaller-crumb rubber particles showed higher energy dissipation. The stiffness reduction in ballast on rubber addition was higher for rigid subgrade.	[73]	

3. Adequacy of Constitutive Model for TDA

This section covers a numerical assessment of the effectiveness of a range of constitutive models to reproduce the laboratory-measured performance of TDA in terms of vertical strain. In this regard, a uniaxial compression test was simulated in finite element software ABAQUS [74] and calibrated against the previous experimental work of Meles et al. [75]. In the literature, the unit weight of TDA was reported to be within the range of 3.4–9.1 kN/m³ depending on the compaction energy, viz., no compaction, light compaction, laboratory compaction, or field compacted [22]. The compaction energy influenced the unit weight of TDA up to 60% of standard proctor compaction energy; after that, the effect was the least [76]. In the present study, the unit weight of the tested TDA was 6.5 kN/m³, which represents the level of compaction adopted for TDAs in practice and was adopted by Meles et al. [75]. Subsequently, the relative density of the tested specimen was 76%, based on maximum and minimum unit weights of 9.1 and 3.4 kN/m³, respectively.

A concentrated load of 510 kN was applied at the top centre of the compression cell, shown in Figure 2a. The base of the compression cell was fixed, and the sides were restricted from movement in the x and y directions. The mesh size of each element was 0.025 m. The total amounts of elements and nodes were 26055 and 28336, respectively. The elements were modelled as eight-noded hexahedral linear brick elements with reduced integration (C3D8R).

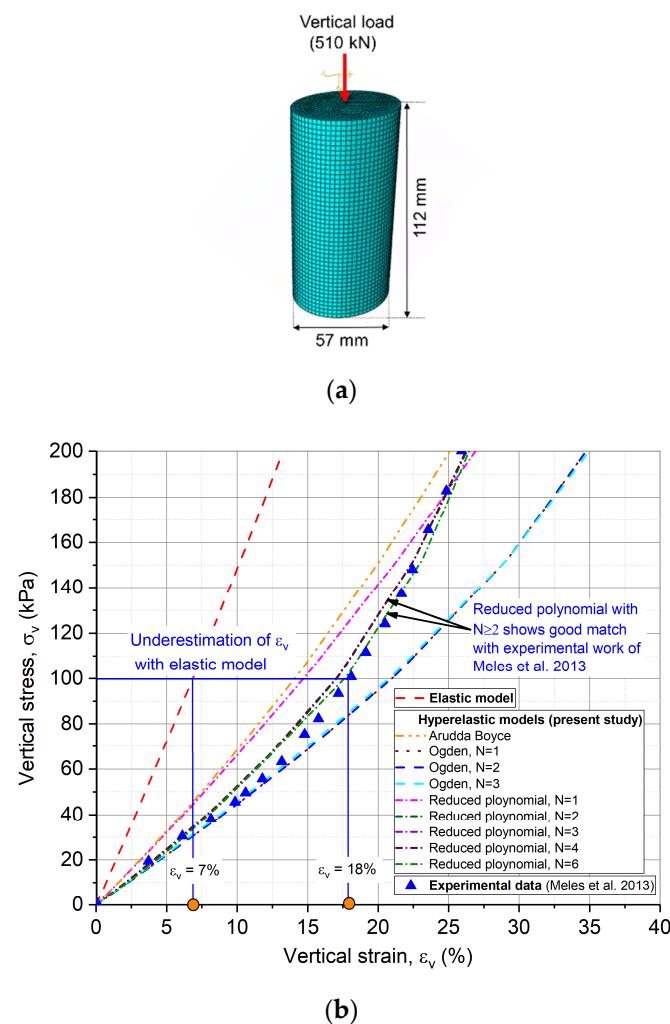


Figure 2. (a) Three-dimensional finite element model of uniaxial compression test. (b) Influence of different constitutive models of TDA on the vertical strain and validation (data sourced from Meles et al. [75]).

It is shown in Figure 2 that the adoption of an elastic constitutive model for TDA leads to the underestimation of vertical strain for a particular value of vertical stress. For example, in Figure 2b, with a vertical stress of 100 kPa, the vertical strain when considering TDA as elastic material is 7%, significantly less than the actual vertical strain of 18% measured experimentally by Meles et al. [75]. Hence, it becomes essential to use a suitable constitutive model for TDA that can correctly predict vertical strain. Hyperelastic is one such type of material model used for rubberlike materials. A hyperelastic model is a nonlinear material model in which large strains can be applied. The material state in a hyperelastic model considers the current loading and is not influenced by history or deformation rate. Various types of hyperelastic models (or forms of the strain energy potential) are available in ABAQUS, viz., polynomial ($N = 1$ (Mooney–Rivlin) and $N = 2$)), Ogden ($N = 1$ to 6), reduced polynomial ($N = 1$ to 6, ($N = 1$ and 3 are called Neo Hooke and Yeoh, respectively)), Arruda–Boyce, Van Der Waals, and Marlow. All these forms constitute incompressible or almost incompressible models. Stability analysis was performed using different hyperelastic constitutive models available in ABAQUS, and the results are plotted for all the stable models in Figure 2b. Generally, it can be seen that the vertical strain predicted by various hyperelastic models compares well with the experimental work of Meles et al. [75]. Arruda–Boyce underestimates the vertical strain, while Ogden overestimates the vertical strain. The reduced polynomial strain energy potential functions with $N = 1$ show similar stress–strain behaviour to Arruda–Boyce. Reduced polynomial strain energy potential functions with $N \geq 2$ depict an excellent match with the experimental work of Meles et al. [75]. The higher the degree of the reduced polynomial, the better the match with experimental work. A reduced polynomial strain energy potential with $N = 3$ (Yeoh model) was chosen for the present study to strike a balance between accuracy and analysis time.

The selection of a suitable constitutive model for TDA is essential to precisely analyse the behaviour of the railway track containing TDA. Figure 3 shows the comparison of vertical elastic displacement (δ_{ev}) and vertical plastic displacement (δ_{pv}) when considering TDA as an elastic and hyperelastic material. The δ_{ev} and δ_{pv} values are reported at the end of the tenth load cycle for comparison purposes. It can be seen that δ_{ev} and δ_{pv} values are underestimated by 43.5% and 30.4%, respectively, when simulating TDA as an elastic material for a ballasted track. Likewise, for a slab track, the δ_{ev} and δ_{pv} values are underestimated by 59.2% and 42.4%, respectively.

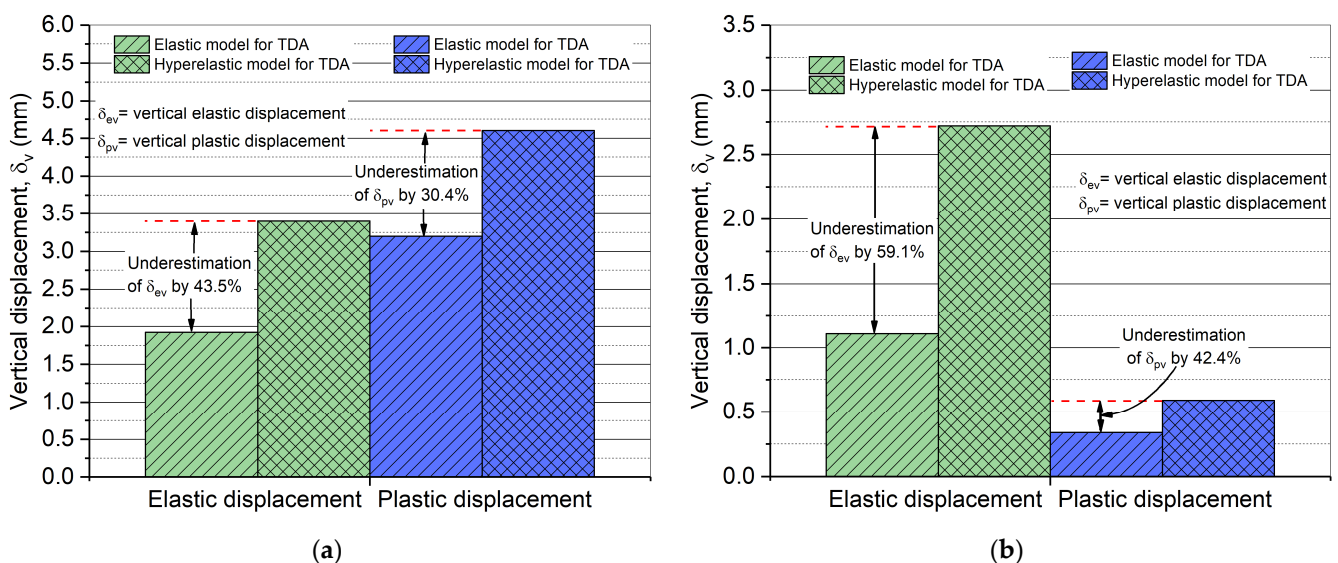


Figure 3. Comparison of elastic and plastic displacements considering TDA as elastic and hyperelastic material for (a) ballasted track and (b) slab track.

4. Stress Transfer in Ballasted and Slab Tracks, with and without TDA

4.1. Methodology

The finite element models of the ballasted and slab tracks adopted in the present study are shown in Figure 4. The steel (rail) and concrete (sleepers, slab, groutmass or cement asphalt mortar layer, and base layer) are modelled as elastic materials as reported by previous studies [60,77]. In the present study, the elastic modulus (E) of concrete used in the hydraulically bonded layer (HBL) was 7.5 GPa, while E for the concrete slab was 20 GPa. Concrete used in the concrete slab and base layer (hydraulically bonded layer) was made of C45/55 and C10/12 mix, respectively (according to BS EN 206:2013 [78], C45/55 means minimum characteristic cylinder strength is 45 MPa and minimum characteristic cube strength is 55 MPa) [79]. The ballast and subballast in a ballasted track and subbase layer in a slab track were modelled as elastoplastic materials with the Drucker–Prager yielding criterion. The subgrade in both track types was modelled as linear elastic/perfectly plastic material adhering to the Mohr–Coulomb failure criterion. The parts were modelled using eight-noded hexahedral linear brick elements with reduced integration (C3D8R). The total elements in the ballasted and slab tracks were 15262 and 15116, respectively. Both track models were restricted from displacements in the x , y , and z directions and a pinned support boundary was applied to the base of the models. The finer mesh was used for top layers, and mesh fineness was reduced from top to bottom to reduce the analysis time and focus more computational efforts on the top layers. Surface-to-surface contact with normal contact as “hard” and tangential behaviour as “penalty (friction coefficient = 0.5)” were used to model the interaction between various layers. The rail and sleeper were connected to a rail pad, which was modelled as a spring (stiffness = 22.5 kN/mm). The elastic material properties of ballasted and slab tracks adopted in the present study are shown in Table 3. The strength properties of both track types are shown in Table 4. The damping ratio was input in ABAQUS using Rayleigh coefficients (α and β), which were determined using Equations (1) and (2), respectively [80]:

$$\alpha = \frac{2\zeta\omega_1\omega_2}{\omega_1 + \omega_2} \quad (1)$$

$$\beta = \frac{2\zeta}{\omega_1 + \omega_2} \quad (2)$$

where ζ is the damping ratio and ω_1 and ω_2 are the angular frequencies for a frequency interval with viscous damping equal to or less than ζ .

Table 3. Elastic material properties used in a numerical model of ballasted and slab tracks (data sourced from [79]).

Material	Constitutive Model		Density, ρ (kg/m ³)		Elastic Modulus, E (MPa)		Poisson's Ratio, ν	
	Ballasted Track	Slab Track	Ballasted Track	Slab Track	Ballasted Track	Slab Track	Ballasted Track	Slab Track
Rail	LE ¹	LE ¹	7830	7830	210,000	210,000	0.3	0.3
Sleeper	LE ¹		2400		30,000		0.15	
Concrete slab		LE ¹		2700		20,000		0.167
Groutmass		LE ¹		2250		27,000		0.167
Ballast	DP ²		1600		110		0.3	
Base (HBL ⁴)		LE ¹		2700		7500		0.167
Subballast/subbase	DP ²	DP ²	2220	2220	400	400	0.25	0.25
Subgrade	MC ³	MC ³	2220	2220	400	400	0.25	0.25

¹ Linear elastic; ² Drucker–Prager; ³ Mohr–Coulomb; ⁴ hydraulically bonded layer.

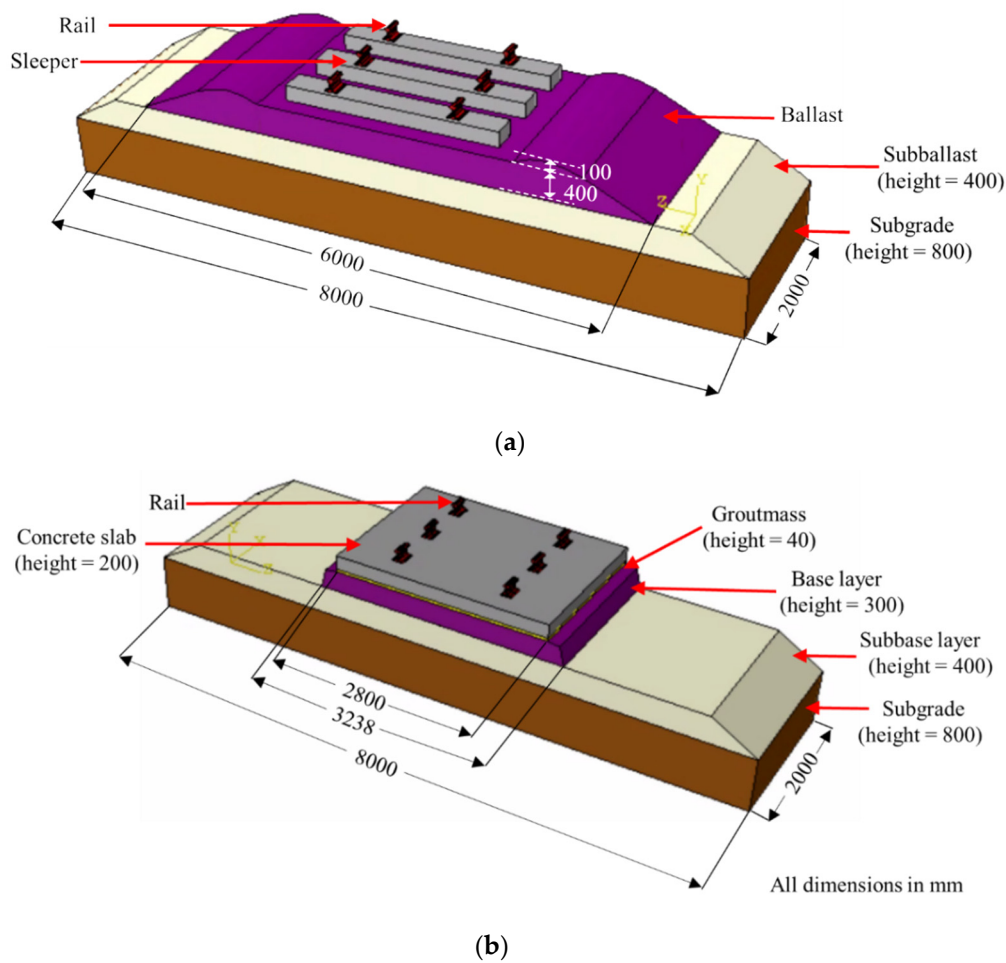


Figure 4. Isometric view of models developed in ABAQUS: (a) ballasted track; (b) slab track.

Previous studies by Fox et al. [23] and McCartney et al. [81] recommend a damping ratio of 18–21% and 16–26.8%, respectively, for TDA. Hence, 20% was adopted as the damping ratio in the present study for the TDA layer. The corresponding α and β for TDA were 7.76 and 0.00299, respectively.

Table 4. Strength properties and damping ratio used in a numerical model of ballasted and slab tracks (data sourced from [79,82]).

Material	Cohesion, c (kPa)		Friction Angle, ϕ ($^\circ$)		Dilation Angle, ψ ($^\circ$)		Damping Ratio, ζ	
	Ballasted Track	Slab Track	Ballasted Track	Slab Track	Ballasted Track	Slab Track	Ballasted Track	Slab Track
Ballast			40		5		0.04 ⁵	
Subballast/subbase	5	5	35 ⁴	35 ⁴	2	2	0.04 ⁵	0.04 ⁵
Subgrade	5	5	35 ⁴	35 ⁴	2	2	0.04 ⁵	0.04 ⁵

⁴ Cebasek et al. [79]; ⁵ Hall [82].

The stress transfer in ballasted and slab tracks with depth was analysed for different train speeds and axle loads. To study the effect of train speed and axle load, only one parameter, viz., train speed or axle load, was varied, whereas the other was constant. A TDA thickness of 25 mm was used for the simulations, and TDA was placed below the subballast and base layers of ballasted and slab tracks, respectively (Figure 5).

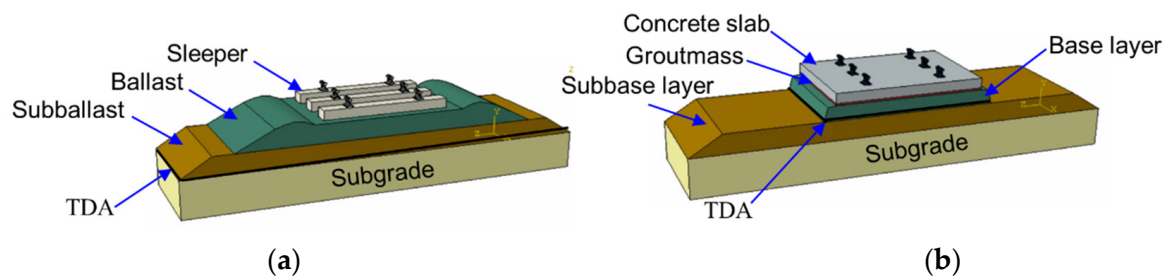


Figure 5. Location of TDA placement for (a) ballasted track and (b) slab track.

The finite element models of ballasted and slab tracks are shown in Figure 6, depicting the vertical displacements upon cyclic load application. The figures on the left side indicate the vertical displacements before the gravity stage application. The figures on the right side represent vertical displacements due to gravity and cyclic load. It can be seen that the maximum vertical rail displacement in a ballasted track is 5 mm, much higher compared to the maximum vertical displacement of 0.07 mm in a slab track.

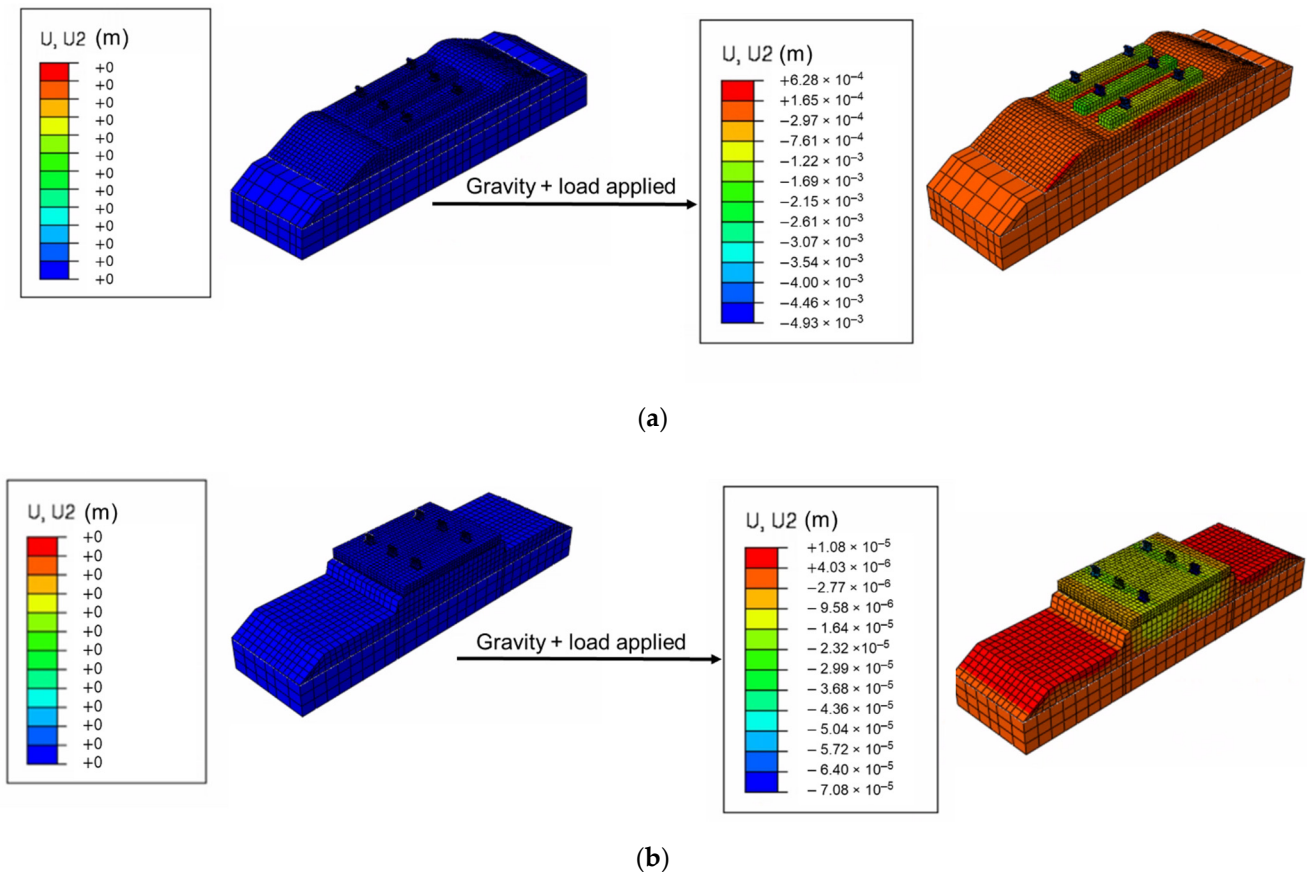


Figure 6. Vertical displacement contour for (a) ballasted track and (b) slab track.

4.2. Validation

The three-dimensional models of the ballasted and slab tracks were validated against the previous experimental work of Cebasek et al. [79]. The predictions of the numerical model were compared against the past experimental work of Cebasek et al. [79] and showed a good match, as shown in Table 5.

Table 5. Comparison of elastic and plastic displacements for ballasted and slab tracks against experimental work.

Displacement	Cebasek et al. [79]		Present Study	
	Ballasted Track	Slab Track	Ballasted Track	Slab Track
Elastic displacement (mm)	0.75	0.053	0.9	0.051
Plastic displacement ¹ (mm)	7.42	0.32	7.86	0.295

¹ Plastic displacement (cumulative settlement) obtained at end of 1.2×10^6 loading cycles.

4.3. Variation in Shear Stress and Displacement with Depth for Ballasted and Slab Tracks

The variation in shear stress values S_{xy} , S_{xz} , and S_{yz} with depth for ballasted and slab tracks (with and without TDA) is illustrated using radar graphs in Figures 7 and 8, respectively. It can be seen that the addition of TDA leads to increases in shear stress (S_{xy} , S_{xz} and S_{yz}) on the sleeper top ($z = 0$) for the ballasted track, while there is a reduction in shear stress on the slab track due to TDA incorporation. The S_{xy} at lower layers of the ballasted track, that is, subgrade top ($z = 1$ m) and bottom ($z = 1.8$ m), reduces by 96.5% and 87.5%, respectively, on TDA incorporation. However, not much change is observed in S_{xz} and S_{yz} after TDA addition. The maximum reduction in shear stress (S_{yz}) for the lower layers of a slab track is around 67% and 46% at subgrade top ($z = 0.94$ m) and bottom ($z = 1.74$ m), respectively, after TDA incorporation.

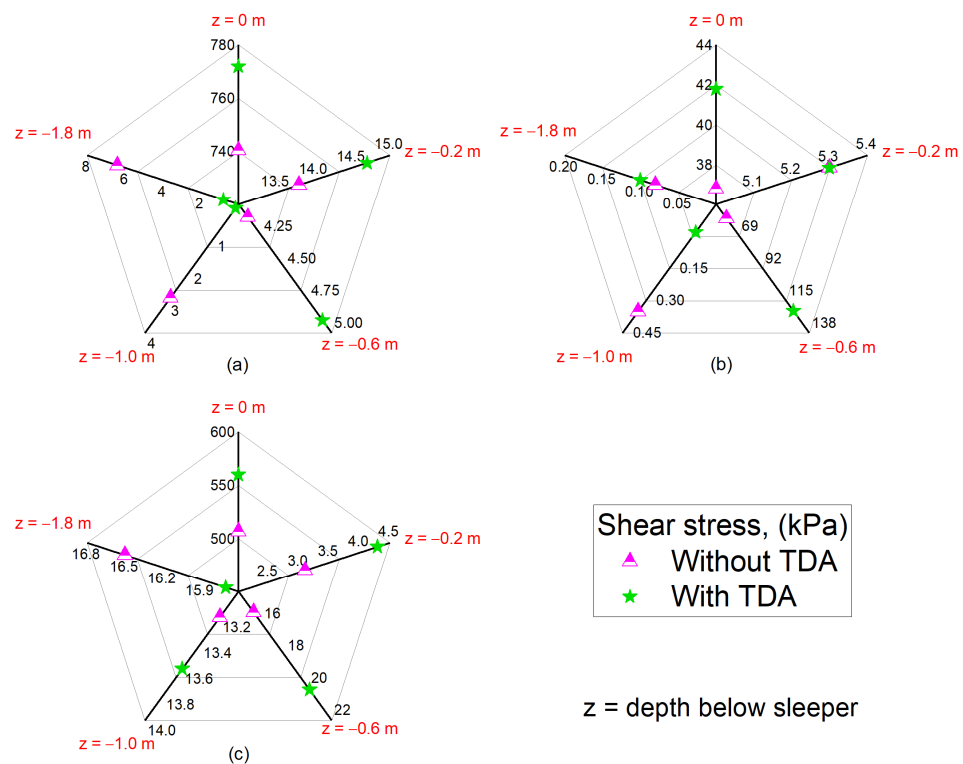


Figure 7. Variation in shear stress (a) S_{xy} , (b) S_{xz} , and (c) S_{yz} with depth (z) below sleeper of a ballasted track.

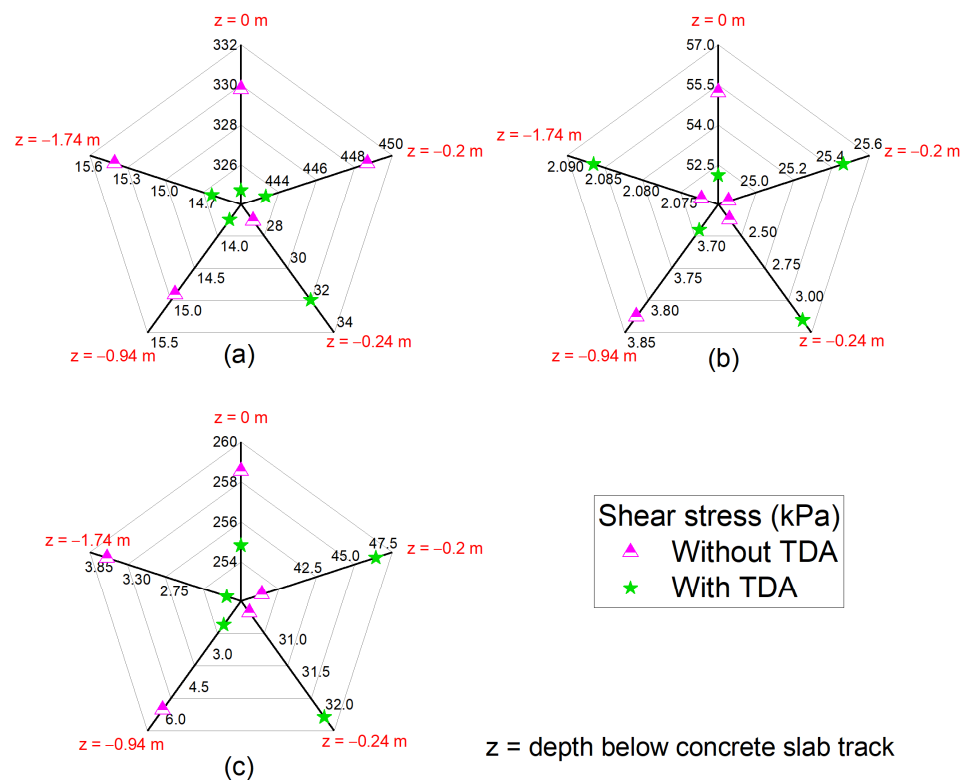


Figure 8. Variation in shear stress (a) S_{xy} , (b) S_{xz} , and (c) S_{yz} with depth (z) below the concrete slab of a slab track.

Figure 9 illustrates the variation in vertical displacement (U_y) with time for ballasted and slab tracks at train speeds of 360 km/h. The train speeds were simulated using different cyclic loading frequencies. It is seen from Figure 9 that the vertical elastic displacements ($U_{e,y}$) for ballasted and slab tracks are 0.9 and 0.05 mm, respectively. The variation in elastic displacements $U_{e,x}$, $U_{e,y}$, and $U_{e,z}$ with depth for ballasted and slab tracks (with and without TDA) is illustrated using radar graphs in Figures 10 and 11, respectively. $U_{e,x}$, $U_{e,y}$, and $U_{e,z}$ represent the elastic displacements in the x , y , and z directions. The maximum elastic displacement occurs in the y (vertical) direction for both track types. The displacements $U_{e,x}$, $U_{e,y}$, and $U_{e,z}$ at different depths of ballasted and slab tracks increase with TDA incorporation, except at subgrade bottom for a ballasted track and subgrade top and subgrade bottom for a slab track. Although displacements increase due to TDA incorporation, they are within the displacement limit of 9 mm [83], and this higher elastic displacement will lead to higher damping and lower track vibrations. The reduction in $U_{e,y}$ for the slab track after TDA addition is 18% and 25% at subgrade top ($z = -0.94$ m) and bottom ($z = -1.74$ m), respectively.

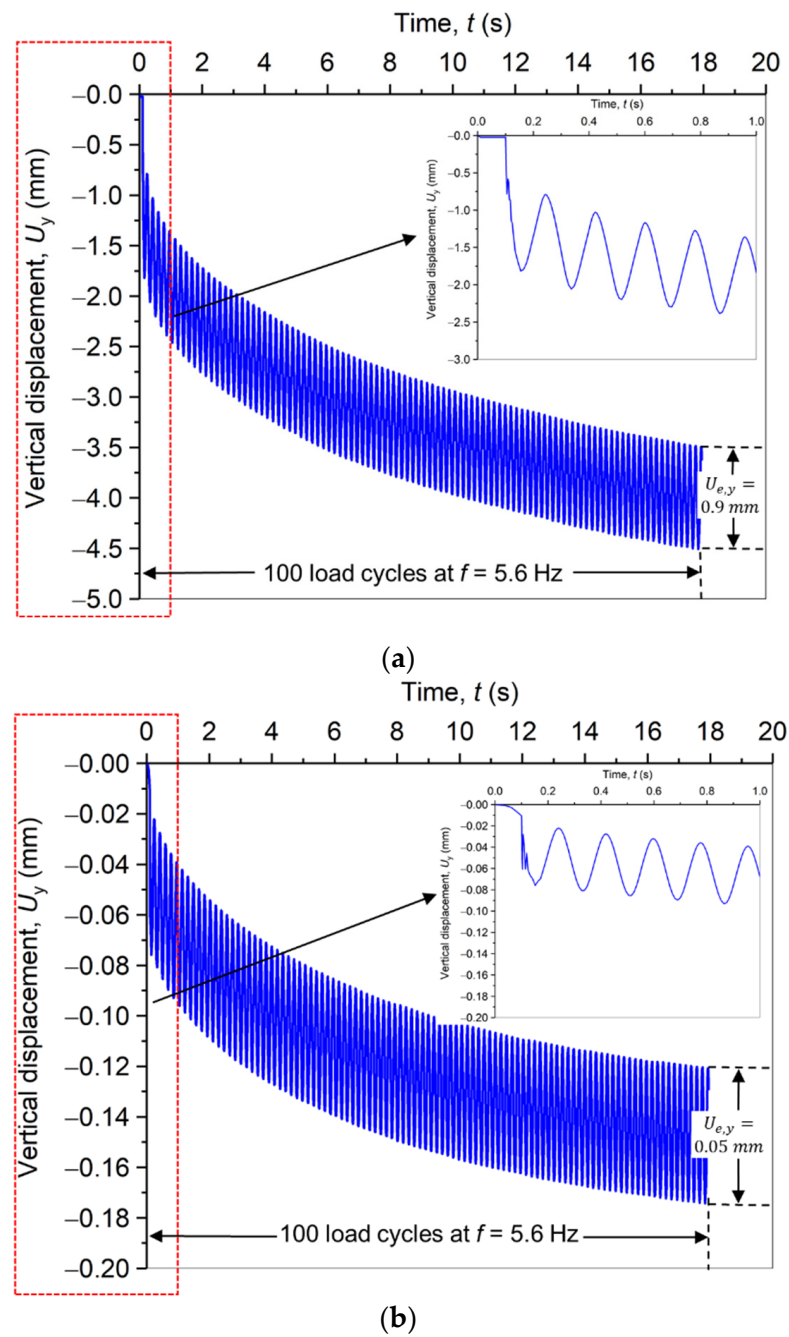


Figure 9. Variation in vertical displacement with time for (a) sleeper of a ballasted track and (b) concrete slab of a slab track, at train speed of 360 km/h ($f = 5.6$ Hz).

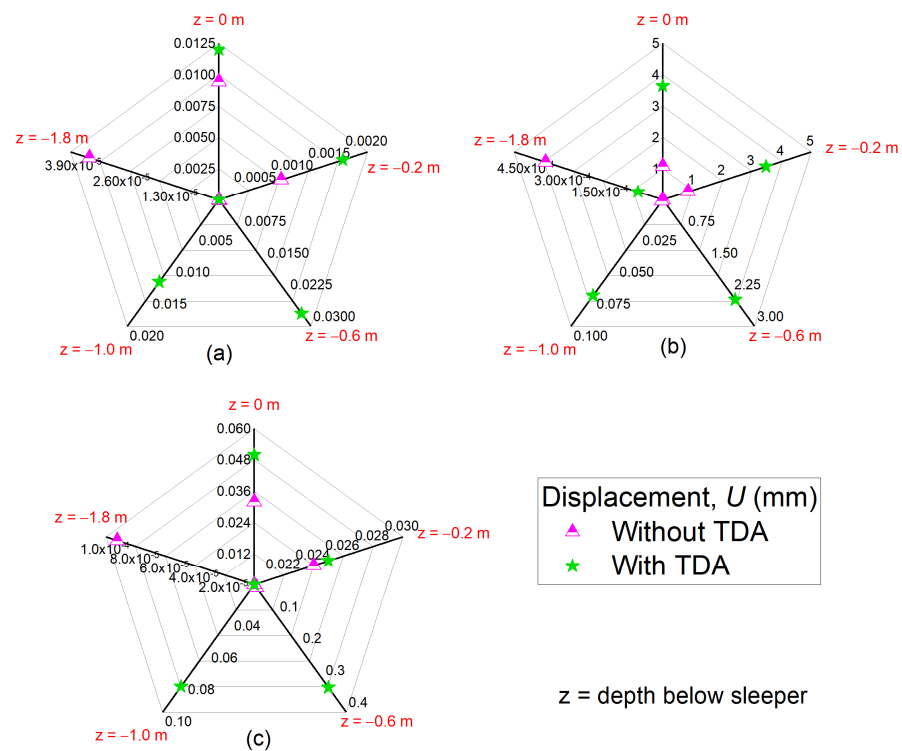


Figure 10. Variation in elastic displacement (a) $U_{e,x}$, (b) $U_{e,y}$, and (c) $U_{e,z}$ with depth (z) below sleeper of a ballasted track.

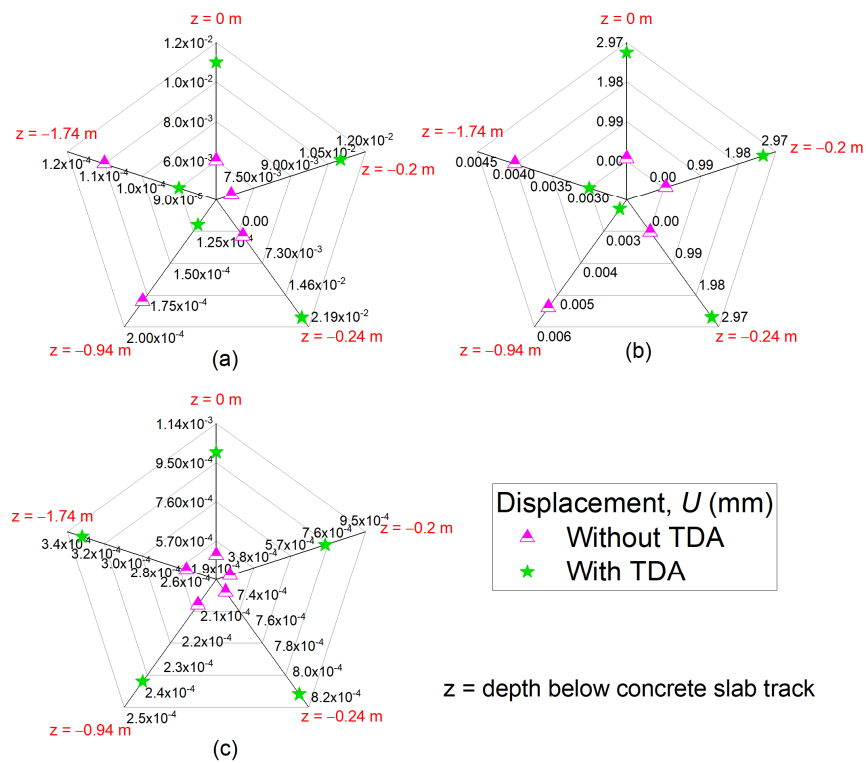


Figure 11. Variation in elastic displacement (a) $U_{e,x}$, (b) $U_{e,y}$, and (c) $U_{e,z}$ with depth (z) below concrete slab of a slab track.

4.4. Effect of Train Speed

The present study considered the train speeds of 160, 260, 360, and 450 km/h, representing loading frequencies of 2.5, 4, 5.6, and 7 Hz, respectively. The frequency is calculated as the ratio of train speed to the vehicle geometry (or wavelength). This wavelength can be passenger car length (λ_{pc}), axle spacing (λ_a), or bogie spacing (λ_b), as shown in Figure 12. In the present study, λ_b was used to calculate the train speed. Figures 13 and 14 show the variation in vertical stress (σ_v) and lateral stress (σ_h) with the depth for ballasted and slab tracks, respectively. It is evident from Figures 13 and 14 that overall both σ_v and σ_h reduce with depth in both track types. In addition, train speed has a negligible influence on σ_v at various depths in both track types. Referring to Figures 13a and 14a, the incorporation of TDA seems to have marginally increased σ_v but substantially increased σ_h in the upper layers of the ballasted track for different train speeds. The addition of TDA helps to reduce σ_v by approximately 30 kPa in a ballasted track near the zone of TDA placement.

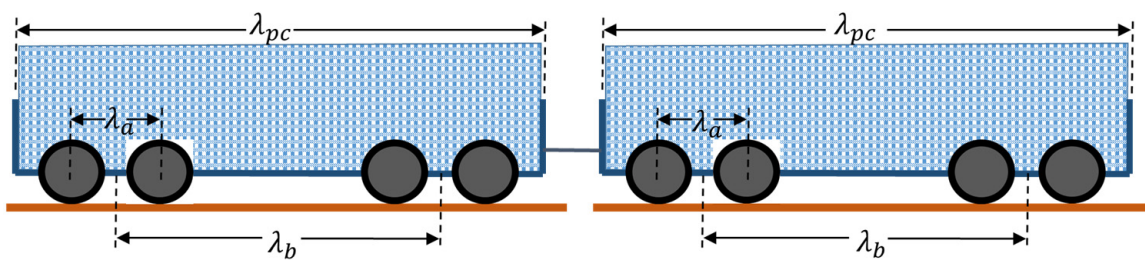
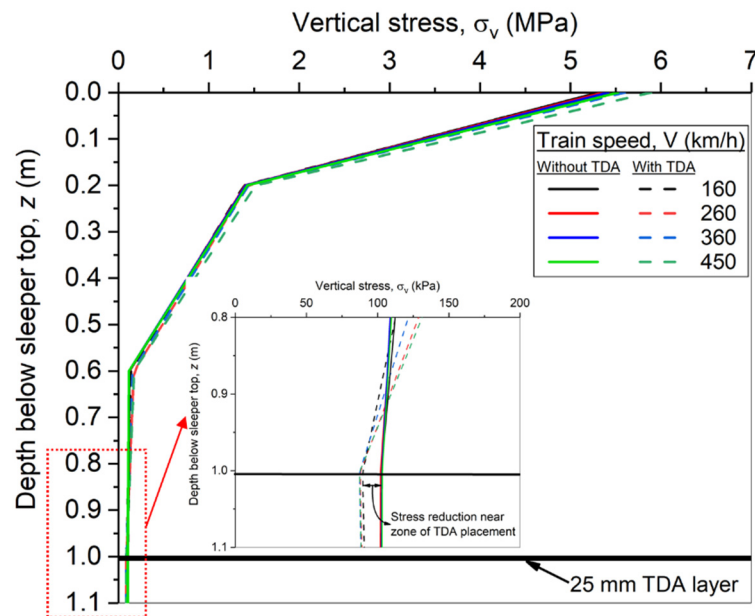


Figure 12. Representation of passenger cars with different types of wavelengths used to calculate train speed.



(a)

Figure 13. Cont.

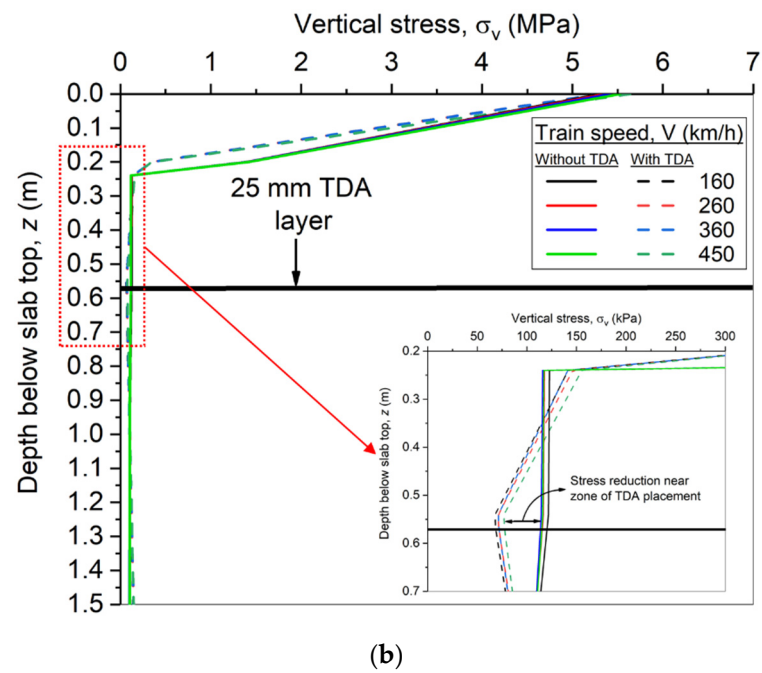


Figure 13. Variation in vertical stress with depth for different train speeds below sleeper top and slab top of (a) ballasted and (b) slab tracks, respectively.

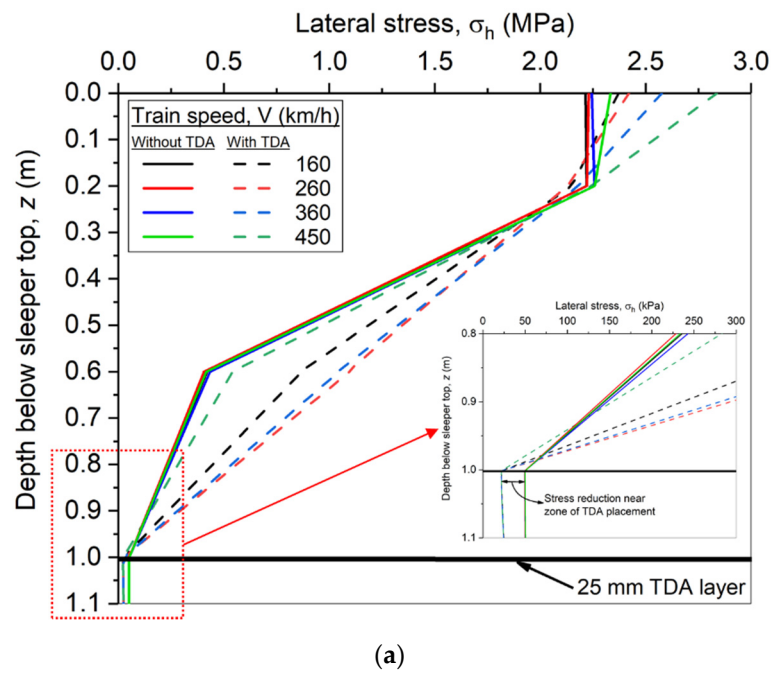


Figure 14. Cont.

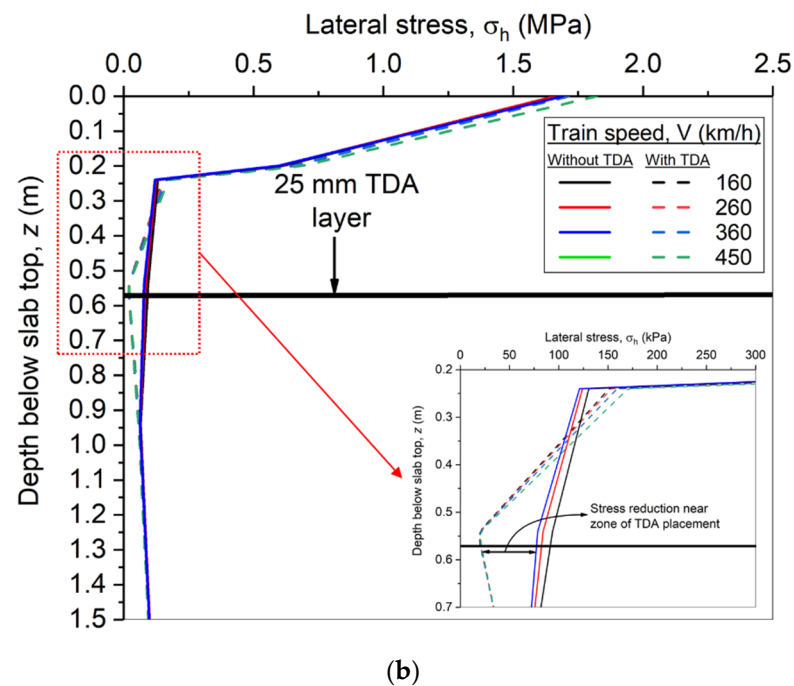


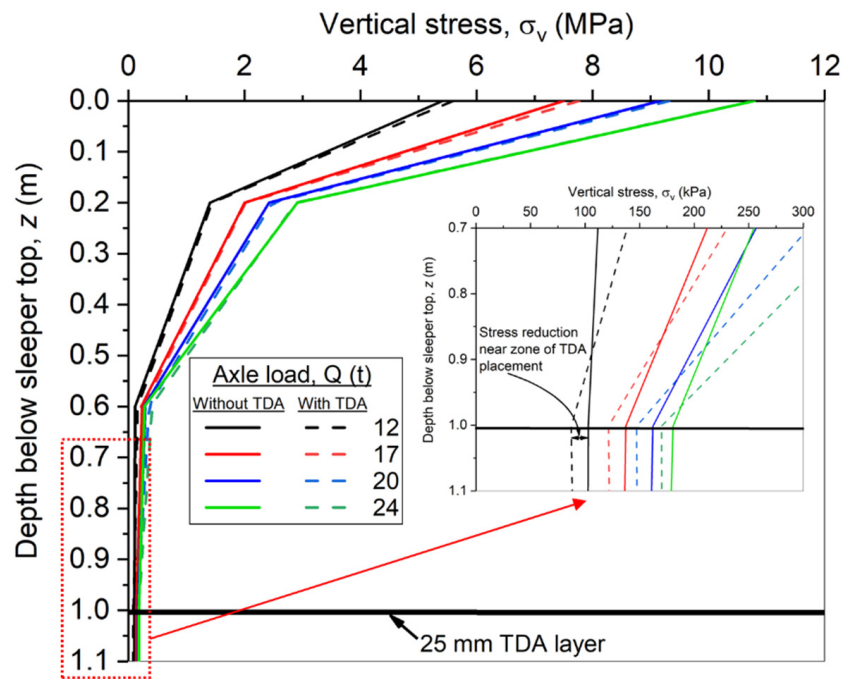
Figure 14. Variation in lateral stress with depth for different train speeds below sleeper top and slab top of (a) ballasted and (b) slab tracks, respectively.

Referring to Figures 13b and 14b, σ_v is lower with TDA incorporation in the upper layers of the slab track. In addition, there is a substantial reduction in the σ_v near the zone of TDA placement. On the other side, σ_h shows a reverse trend for the upper layers of the slab track with TDA addition, but near the zone of TDA placement, a reduction in σ_h (more than 50 kPa) is observed.

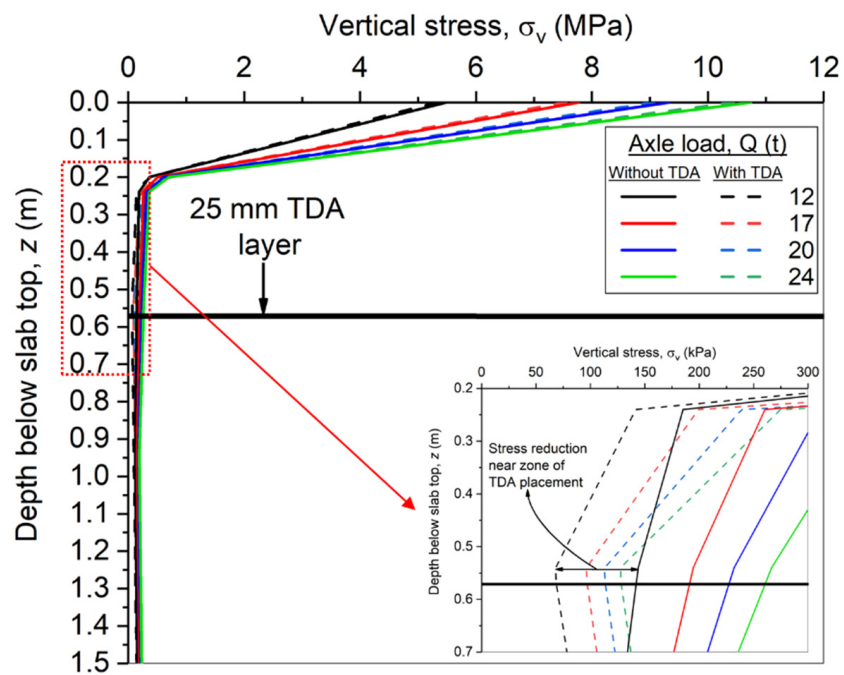
4.5. Effect of Axle Load

The axle loads of 12, 17, 20, and 24 t were considered in the present study, representing the axle load of passenger trains commonly used in practice. Figures 15 and 16 illustrate the variation in σ_v and σ_h with depth for ballasted and slab tracks, respectively. Generally, both σ_v and σ_h increase with increasing axle loads for both track types. In a ballasted track, the incorporation of TDA slightly enhances σ_v in the top layers while a reduction in σ_v is noticed in the subgrade near the zone of TDA placement, as shown in Figure 15a. The σ_h in the upper layers of the ballasted track increases with TDA incorporation for lower axle loads of 12 t, reduces at axle loads of 17 t, and remains almost the same for axle loads of 20 and 24 t, as shown in Figure 16a. In addition, a reduction in σ_h is observed near the zone of TDA placement with a higher reduction for higher axle loads.

Referring to Figures 15b and 16b, the addition of TDA has the most negligible influence on σ_v and σ_h in the upper layers of the slab track. However, there is a 60% reduction in σ_v near the TDA placement zone, and this reduction increases for higher axle loads. Similarly, more than a 60% reduction in σ_h is recorded for the slab track near the region of TDA placement.



(a)



(b)

Figure 15. Variation in vertical stress with depth for different axle loads below sleeper top and slab top of (a) ballasted and (b) slab tracks, respectively.

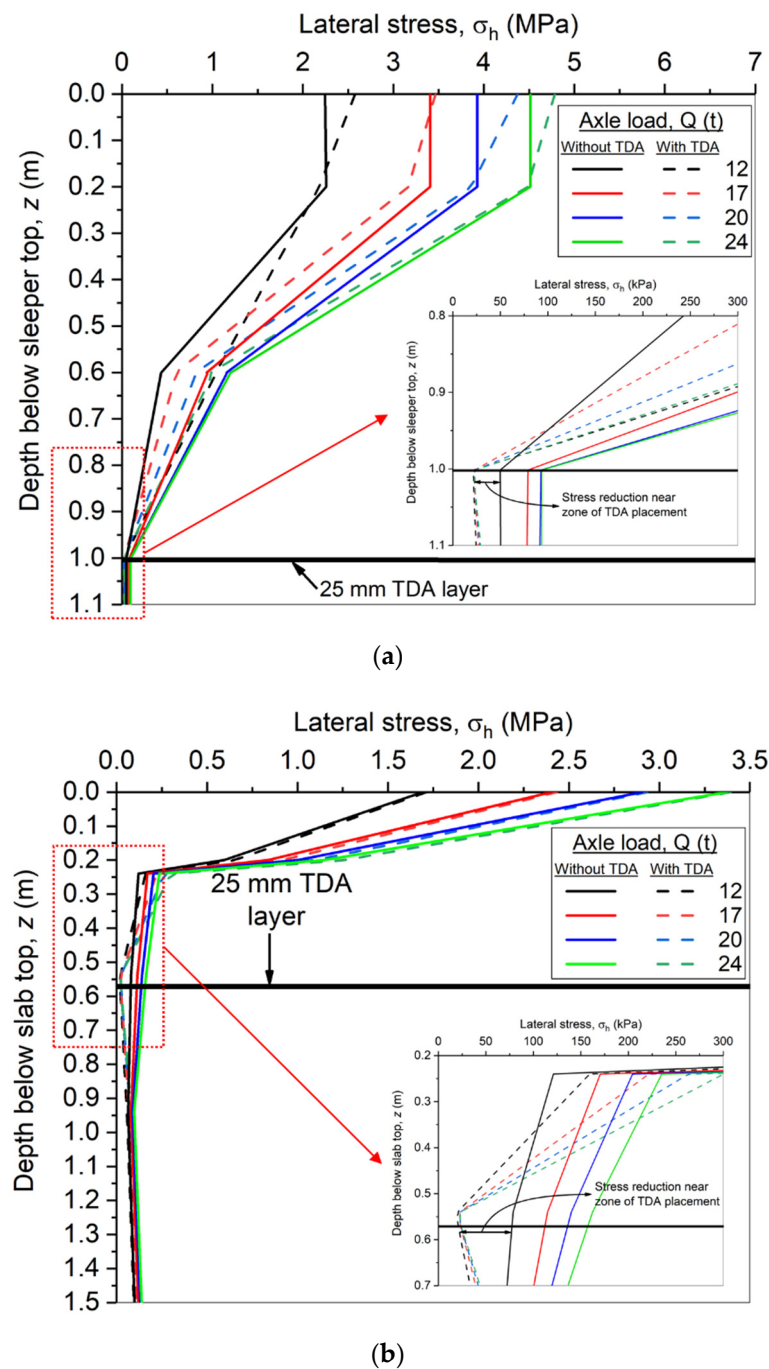


Figure 16. Variation in lateral stress with depth for different axle loads below sleeper top and slab top of (a) ballasted and (b) slab tracks, respectively.

5. Conclusions

The present study sheds light on the significant benefits associated with rubber recycling, viz., the conservation of landfill space, reduction in environmental pollution, and creation of new products. The applications of scrap rubber in civil engineering projects have been elaborated upon. Generally, scrap tyres have shown excellent performance as fill material, backfill material, and drainage layers. Most importantly, scrap tyres help to reduce vibration levels on a railway track.

This study highlights the importance of adopting a hyperelastic constitutive model for TDA. It is observed that vertical elastic and plastic displacements are underestimated by 59.2% and 42.4%, respectively, when simulating TDA as an elastic material for a slab track.

Similarly, the vertical elastic and plastic displacements are underestimated by 43.5% and 30.4% for a ballasted track, respectively. The shear stress results show that the addition of TDA helps to reduce the shear stress on the concrete slab of slab track, while shear stresses are increased for a ballasted track after rubber incorporation. However, TDA effectively reduces shear stresses for the lower layer of both track types. The elastic displacements (U_x , U_y , and U_z) at different depths of ballasted and slab tracks increase with TDA incorporation except on subgrade layers. Scrap rubber helps reduce the vertical and lateral stress near the zone of its placement in ballasted and slab tracks for varying train speeds. Train speed has a negligible influence on vertical stress at various depths in both track types. The lateral stress in a ballasted track is influenced by train speed, while the impact is less pronounced in a slab track. Scrap rubber is more effective in reducing vertical and lateral stress near the region of its placement for higher axle loads.

Author Contributions: Conceptualisation, M.A.F. and S.N.; methodology, M.A.F. and S.N.; software, M.A.F.; validation, M.A.F.; formal analysis, M.A.F. and S.N.; investigation, M.A.F. and S.N.; data curation, M.A.F. and S.N.; writing—original draft preparation, M.A.F.; writing—review and editing, S.N. and B.F.; supervision, S.N. and B.F.; project administration, S.N. All authors have read and agreed to the published version of the manuscript.

Funding: This research received no external funding.

Institutional Review Board Statement: Not applicable.

Informed Consent Statement: Not applicable.

Data Availability Statement: The data presented in this study are available on request from the corresponding author. The data are not publicly available as research is still in progress.

Acknowledgments: This research was financially supported by Australian Government Research Training Program.

Conflicts of Interest: The authors declare no conflict of interest.

References

- Arulrajah, A.; Naeini, M.; Mohammadinia, A.; Horpibulsuk, S.; Leong, M. Recovered Plastic and Demolition Waste Blends as Railway Capping Materials. *Transp. Geotech.* **2020**, *22*, 100320. [CrossRef]
- Qi, Y.; Indraratna, B.; Heitor, A.; Vinod, J.S. Effect of Rubber Crumbs on the Cyclic Behavior of Steel Furnace Slag and Coal Wash Mixtures. *J. Geotech. Geoenviron. Eng.* **2018**, *144*, 04017107. [CrossRef]
- Naeini, M.; Mohammadinia, A.; Arulrajah, A.; Horpibulsuk, S.; Leong, M. Stiffness and Strength Characteristics of Demolition Waste, Glass and Plastics in Railway Capping Layers. *Soils Found.* **2019**, *59*, 2238–2253. [CrossRef]
- Yoon, S.; Prezzi, M.; Siddiki, N.Z.; Kim, B. Construction of a Test Embankment Using a Sand–Tire Shred Mixture as Fill Material. *Waste Manag.* **2006**, *26*, 1033–1044. [CrossRef] [PubMed]
- Farooq, M.A.; Nimbalkar, S.; Fatahi, B. Three-Dimensional Finite Element Analyses of Tyre Derived Aggregates in Ballasted and Ballastless Tracks. *Comput. Geotech.* **2021**, *136*, 104220. [CrossRef]
- Asadi, M.; Mahboubi, A.; Thoani, K. Discrete Modeling of Sand–Tire Mixture Considering Grain-Scale Deformability. *Granul. Matter* **2018**, *20*, 18. [CrossRef]
- Ghazavi, M. Shear Strength Characteristics of Sand-Mixed with Granular Rubber. *Geotech. Geol. Eng.* **2004**, *22*, 401–416. [CrossRef]
- Akbas, A.; Yuhana, N.Y. Recycling of Rubber Wastes as Fuel and Its Additives. *Recycling* **2021**, *6*, 78. [CrossRef]
- Feraldi, R.; Cashman, S.; Huff, M.; Raahauge, L. Comparative LCA of Treatment Options for US Scrap Tires: Material Recycling and Tire-Derived Fuel Combustion. *Int. J. Life Cycle Assess.* **2013**, *18*, 613–625. [CrossRef]
- Vishnu, T.B.; Singh, K.L. A Study on the Suitability of Solid Waste Materials in Pavement Construction: A Review. *Int. J. Pavement Res. Technol.* **2021**, *14*, 625–637. [CrossRef]
- Rodríguez, L.M.; Arroyo, M.; Cano, M.M. Use of Tire-Derived Aggregate in Tunnel Cut-and-Cover. *Can. Geotech. J.* **2018**, *55*, 968–978. [CrossRef]
- Waste Management Review A Rubbery Problem—The Australian Scrap Tyre Management Challenge. Available online: <https://wastemanagementreview.com.au/a-rubbery-problem/%0A> (accessed on 23 November 2021).
- Thomas, B.S.; Gupta, R.C. A Comprehensive Review on the Applications of Waste Tire Rubber in Cement Concrete. *Renew. Sustain. Energy Rev.* **2016**, *54*, 1323–1333. [CrossRef]
- Kaneko, T.; Orense, R.P.; Hyodo, M.; Yoshimoto, N. Seismic Response Characteristics of Saturated Sand Deposits Mixed with Tire Chips. *J. Geotech. Geoenviron. Eng.* **2013**, *139*, 633–643. [CrossRef]

15. ISRI. The Facts about Recycled Rubber. Available online: https://www.recycledrubberfacts.org/wp-content/uploads/2016/03/Recycled_Rubber_Brochure.pdf (accessed on 16 June 2022).
16. Jamshidi Chenari, R.; Fatahi, B.; Akhavan Maroufi, M.A.; Alaie, R. An Experimental and Numerical Investigation into the Compressibility and Settlement of Sand Mixed with TDA. *Geotech. Geol. Eng.* **2017**, *35*, 2401–2420. [[CrossRef](#)]
17. Gong, H.; Song, W.; Huang, B.; Shu, X.; Han, B.; Wu, H.; Zou, J. Direct Shear Properties of Railway Ballast Mixed with Tire Derived Aggregates: Experimental and Numerical Investigations. *Constr. Build. Mater.* **2019**, *200*, 465–473. [[CrossRef](#)]
18. Ni, P.; Qin, X.; Yi, Y. Numerical Study of Earth Pressures on Rigid Pipes with Tire-Derived Aggregate Inclusions. *Geosynth. Int.* **2018**, *25*, 494–506. [[CrossRef](#)]
19. ASTM D6270; Standard Practice for Use of Scrap Tires in Civil Engineering Applications. ASTM: West Conshohocken, PA, USA, 2017. [[CrossRef](#)]
20. Matthews, M. Review of Management of Used Tyres at Landfill Sites. *Sustain. Strateg. Solut.* **2006**. Available online: https://www.wasteauthority.wa.gov.au/images/resources/files/2019/11/Review_of_Management_of_Used_Tyres_at_Landfill_Sites.pdf (accessed on 17 June 2022).
21. Ahn, I.S.; Cheng, L.; Fox, P.J.; Wright, J.; Patenaude, S.; Fujii, B. Material Properties of Large-Size Tire Derived Aggregate for Civil Engineering Applications. *J. Mater. Civ. Eng.* **2015**, *27*, 1–11. [[CrossRef](#)]
22. *Geosyntec Guidance Manual for Engineering Use of Scrap Tires*; Proj. No. ME0012-11; Maryland Department of the Environment's Scrap Tire Program: Baltimore, MD, USA, 2008.
23. Fox, P.J.; Thielmann, S.S.; Sanders, M.J.; Latham, C.; Ghaaowd, I.; McCartney, J.S. Large-Scale Combination Direct Shear/Simple Shear Device for Tire-Derived Aggregate. *Geotech. Test. J.* **2018**, *41*, 340–353. [[CrossRef](#)]
24. Rinkesh What Is Rubber Recycling. Available online: <https://www.conserve-energy-future.com/recyclingrubber.php> (accessed on 17 June 2022).
25. Cerminara, G.; Cossu, R. Waste Input to Landfills. In *Solid Waste Landfilling*; Elsevier: Amsterdam, The Netherlands, 2018; pp. 15–39.
26. Ecogreen Benefits of Using Recycling Tires. Available online: <https://ecogreenequipment.com/benefits-of-recycling-tires/> (accessed on 17 June 2022).
27. Alfayez, S.A.; Suleiman, A.R.; Nehdi, M.L. Recycling Tire Rubber in Asphalt Pavements: State of the Art. *Sustainability* **2020**, *12*, 9076. [[CrossRef](#)]
28. Revelo, C.F.; Correa, M.; Aguilar, C.; Colorado, H.A. Composite Materials Made of Waste Tires and Polyurethane Resin: A Case Study of Flexible Tiles Successfully Applied in Industry. *Case Stud. Constr. Mater.* **2021**, *15*, e00681. [[CrossRef](#)]
29. Kaewunruen, S.; Li, D.; Chen, Y.; Xiang, Z. Enhancement of Dynamic Damping in Eco-Friendly Railway Concrete Sleepers Using Waste-Tyre Crumb Rubber. *Materials* **2018**, *11*, 1169. [[CrossRef](#)] [[PubMed](#)]
30. Chowdhury, E.H. Scrap Unused Tyres to Prevent Dengue. Available online: <https://www.daily-sun.com/post/485822/Scrap-unused-tyres-to-prevent-dengue> (accessed on 17 June 2022).
31. Anderson, S. Crews Battle Blaze at Melbourne Tyre Dump. Available online: <https://www.abc.net.au/news/2016-01-11/melbourne-industrial-fire-in-pictures/7080620%0A> (accessed on 17 June 2022).
32. Bosscher, P.J.; Edil, T.B.; Kuraoka, S. Design of Highway Embankments Using Tire Chips. *J. Geotech. Geoenviron. Eng.* **1997**, *123*, 295–304. [[CrossRef](#)]
33. Hoppe, E.J. Field Study of Shredded-Tire Embankment. *Transp. Res. Rec. J. Transp. Res. Board* **1998**, *1619*, 47–54. [[CrossRef](#)]
34. Humphrey, D.N. Tire Derived Aggregate as Lightweight Fill for Embankments and Retaining Walls. In Proceedings of the International Workshop on Scrap Tire Derived Geomaterials, Yokosuka, Japan, 23–24 March 2007; pp. 59–81.
35. Zhang, T.; Cai, G.; Duan, W. Strength and Microstructure Characteristics of the Recycled Rubber Tire-Sand Mixtures as Lightweight Backfill. *Environ. Sci. Pollut. Res.* **2018**, *25*, 3872–3883. [[CrossRef](#)]
36. Tweedie, J.J.; Humphrey, D.N.; Sandford, T.C. Full-Scale Field Trials of Tire Shreds as Lightweight Retaining Wall Backfill under at-Rest Conditions. *Transp. Res. Rec. J. Transp. Res. Board* **1998**, *1619*, 64–71. [[CrossRef](#)]
37. Cecich, V.; Gonzales, L.; Hoisaeter, A.; Williams, J.; Reddy, K. Use of Shredded Tires as Lightweight Backfill Material for Retaining Structures. *Waste Manag. Res. J. Sustain. Circ. Econ.* **1996**, *14*, 433–451. [[CrossRef](#)]
38. Edil, T.B.; Park, J.K.; Kim, J.Y. Effectiveness of Scrap Tire Chips as Sorptive Drainage Material. *J. Environ. Eng.* **2004**, *130*, 824–831. [[CrossRef](#)]
39. Hidalgo-Signes, C.; Garzón-Roca, J.; Grima-Palop, J.M.; Insa-Franco, R. Use of Rubber Shreds to Enhance Attenuation of Railway Sub-Ballast Layers Made of Unbound Aggregates. *Mater. Construcción* **2017**, *67*, 115. [[CrossRef](#)]
40. Wolfe, S.L.; Humphrey, D.N.; Wetzell, E.A. Development of Tire Shred Underlayment to Reduce Ground-Borne Vibration from LRT Track. In *Geotechnical Engineering for Transportation Projects*; ASCE: Reston, VA, USA, 2004; pp. 750–759.
41. Envirologic, I. *A Report on the Use of Shredded Scrap Tires in On-Site Sewage Disposal Systems*; Report to Vermont Department of Environmental Conservation State of Vermont, Recycling Marke, Development Grant; Envirologic Technologies Inc.: Brattleboro, VT, USA, 1990.
42. Hazarika, H.; Kohama, E.; Sugano, T. Underwater Shake Table Tests on Waterfront Structures Protected with Tire Chips Cushion. *J. Geotech. Geoenviron. Eng.* **2008**, *134*, 1706–1719. [[CrossRef](#)]
43. Widayatmoko, I.; Elliot, R. *A Review of the Use of Crumb Rubber Modified Asphalt Worldwide*; Waste and Resources Action Programme: Banbury, UK, 2007.

44. Lo Presti, D. Recycled Tyre Rubber Modified Bitumens for Road Asphalt Mixtures: A Literature Review. *Constr. Build. Mater.* **2013**, *49*, 863–881. [[CrossRef](#)]
45. Adesina, A. Overview of the Influence of Waste Materials on the Thermal Conductivity of Cementitious Composites. *Clean. Eng. Technol.* **2021**, *2*, 100046. [[CrossRef](#)]
46. Shalaby, A.; Khan, A.R. Temperature Monitoring and Compressibility Measurement of a Tire Shred Embankment: Winnipeg, Manitoba, Canada. *Transp. Res. Rec. J. Transp. Res. Board* **2002**, *1808*, 67–75. [[CrossRef](#)]
47. Humphrey, D.; Nickels, W.L., Jr. Tire Chips as Subgrade Insulation and Lightweight Fill. In *Proceedings of the 18th Annual Meeting of the Asphalt Recycling and Reclaiming Association*; Asphalt Recycling and Reclaiming Association: Annapolis, MD, USA, 1994; pp. 83–105.
48. Zornberg, J.G.; Cabral, A.R.; Viratjandr, C. Behaviour of Tire Shred—Sand Mixtures. *Can. Geotech. J.* **2004**, *41*, 227–241. [[CrossRef](#)]
49. Chaney, R.; Demars, K.; Masad, E.; Taha, R.; Ho, C.; Papagiannakis, T. Engineering Properties of Tire/Soil Mixtures as a Lightweight Fill Material. *Geotech. Test. J.* **1996**, *19*, 297. [[CrossRef](#)]
50. Disfani, M.M.; Tsang, H.-H.; Arulrajah, A.; Yaghoubi, E. Shear and Compression Characteristics of Recycled Glass-Tire Mixtures. *J. Mater. Civ. Eng.* **2017**, *29*, 06017003. [[CrossRef](#)]
51. Tatlisoz, N.; Edil, T.B.; Benson, C.H. Interaction between Reinforcing Geosynthetics and Soil-Tire Chip Mixtures. *J. Geotech. Geoenviron. Eng.* **1998**, *124*, 1109–1119. [[CrossRef](#)]
52. Alves Costa, P.; Calçada, R.; Silva Cardoso, A. Ballast Mats for the Reduction of Railway Traffic Vibrations: Numerical Study. *Soil Dyn. Earthq. Eng.* **2012**, *42*, 137–150. [[CrossRef](#)]
53. Nimbalkar, S.; Indraratna, B.; Dash, S.K.; Christie, D. Improved Performance of Railway Ballast under Impact Loads Using Shock Mats. *J. Geotech. Geoenviron. Eng.* **2012**, *138*, 281–294. [[CrossRef](#)]
54. Nimbalkar, S.; Indraratna, B. Improved Performance of Ballasted Rail Track Using Geosynthetics and Rubber Shockmat. *J. Geotech. Geoenviron. Eng.* **2016**, *142*, 04016031. [[CrossRef](#)]
55. Esmaeili, M.; Siahkouhi, M. Tire-Derived Aggregate Layer Performance in Railway Bridges as a Novel Impact Absorber: Numerical and Field Study. *Struct. Control Health Monit.* **2019**, *26*, e2444. [[CrossRef](#)]
56. Fathali, M.; Nejad, F.M.; Esmaeili, M. Influence of Tire-Derived Aggregates on the Properties of Railway Ballast Material. *J. Mater. Civ. Eng.* **2017**, *29*, 04016177. [[CrossRef](#)]
57. Esmaeili, M.; Aela, P.; Hosseini, A. Experimental Assessment of Cyclic Behavior of Sand-Fouled Ballast Mixed with Tire Derived Aggregates. *Soil Dyn. Earthq. Eng.* **2017**, *98*, 1–11. [[CrossRef](#)]
58. Song, W.; Huang, B.; Shu, X.; Wu, H.; Gong, H.; Han, B.; Zou, J. Improving Damping Properties of Railway Ballast by Addition of Tire-Derived Aggregate. *Transp. Res. Rec.* **2019**, *2673*, 299–307. [[CrossRef](#)]
59. Ho, C.; Humphrey, D.; Hyslip, J.; Moorhead, W. Use of Recycled Tire Rubber to Modify Track-Substructure Interaction. *Transp. Res. Rec.* **2013**, *2374*, 119–125. [[CrossRef](#)]
60. Xiao, X.; Wang, J.; Cai, D.; Lou, L.; Xiao, F. A Novel Application of Thermoplastic Polyurethane/Waste Rubber Powder Blend for Waterproof Seal Layer in High-Speed Railway. *Transp. Geotech.* **2021**, *27*, 100503. [[CrossRef](#)]
61. Esmaeili, M.; Ebrahimi, H.; Sameni, M.K. Experimental and Numerical Investigation of the Dynamic Behavior of Ballasted Track Containing Ballast Mixed with TDA. *Proc. Inst. Mech. Eng. Part F J. Rail Rapid Transit* **2018**, *232*, 297–314. [[CrossRef](#)]
62. Towers, D. Evaluation of the Ground-borne Vibration Reduction Properties of Tire-derived Aggregate Installed on the Denver RTD Light Rail System. In *Noise and Vibration Mitigation for Rail Transportation Systems*; Springer: Tokyo, Japan, 2012; pp. 118, 283–290. [[CrossRef](#)]
63. Sol-Sánchez, M.; Moreno-Navarro, F.; Tauste-Martínez, R.; Saiz, L.; Rubio-Gámez, M.C. Recycling Tire-Derived Aggregate as Elastic Particles under Railway Sleepers: Impact on Track Lateral Resistance and Durability. *J. Clean. Prod.* **2020**, *277*, 123322. [[CrossRef](#)]
64. Mehran Khoshoei, S.; Mortazavi Bak, H.; Mahdi Abtahi, S.; Mahdi Hejazi, S.; Shahbodagh, B. Experimental Investigation of the Cyclic Behavior of Steel-Slag Ballast Mixed with Tire-Derived Aggregate. *J. Mater. Civ. Eng.* **2021**, *33*, 04020468. [[CrossRef](#)]
65. Sun, Q. Numerical Simulation of the Dynamic Response of Ballasted Track Overlying a Tire-Reinforced Capping Layer. *Front. Built Environ.* **2020**, *6*, 6. [[CrossRef](#)]
66. Montella, G.; Calabrese, A.; Serino, G. Mechanical Characterization of a Tire Derived Material: Experiments, Hyperelastic Modeling and Numerical Validation. *Constr. Build. Mater.* **2014**, *66*, 336–347. [[CrossRef](#)]
67. Guo, Y.; Shi, C.; Zhao, C.; Markine, V.; Jing, G. Numerical Analysis of Train-Track-Subgrade Dynamic Performance with Crumb Rubber in Ballast Layer. *Constr. Build. Mater.* **2022**, *336*, 127559. [[CrossRef](#)]
68. Guo, Y.; Ji, Y.; Zhou, Q.; Markine, V.; Jing, G. Discrete Element Modelling of Rubber-Protected Ballast Performance Subjected to Direct Shear Test and Cyclic Loading. *Sustainability* **2020**, *12*, 2836. [[CrossRef](#)]
69. Ding, Y.; Zhang, J.; Chen, X.; Wang, X.; Jia, Y. Experimental Investigation on Static and Dynamic Characteristics of Granulated Rubber-Sand Mixtures as a New Railway Subgrade Filler. *Constr. Build. Mater.* **2021**, *273*, 121955. [[CrossRef](#)]
70. Sol-Sánchez, M.; Moreno-Navarro, F.; Saiz, L.; Rubio-Gámez, M.C. Recycling Waste Rubber Particles for the Maintenance of Different States of Railway Tracks through a Two-Step Stoneblowing Process. *J. Clean. Prod.* **2020**, *244*, 118570. [[CrossRef](#)]
71. Yu, P.; Manalo, A.; Ferdous, W.; Abousnina, R.; Salih, C.; Heyer, T.; Schubel, P. Investigation on the Physical, Mechanical and Microstructural Properties of Epoxy Polymer Matrix with Crumb Rubber and Short Fibres for Composite Railway Sleepers. *Constr. Build. Mater.* **2021**, *295*, 123700. [[CrossRef](#)]

72. Esmaeili, M.; Namaei, P. Effect of Mother Rock Strength on Rubber-Coated Ballast (RCB) Deterioration. *Constr. Build. Mater.* **2022**, *316*, 126106. [[CrossRef](#)]
73. Koohmishi, M.; Azarhoosh, A. Stiffness and Damping Properties of Railway Ballast Aggregate Considering Influence of Degradation of Aggregate and Incorporation of Crumb Rubber. *Soil Dyn. Earthq. Eng.* **2022**, *155*, 107177. [[CrossRef](#)]
74. *Dassault Systems ABAQUS*; Dassault Systèmes Simulia Corp: Providence, RI, USA, 2018.
75. Meles, D.; Bayat, A.; Soleymani, H. Compression Behavior of Large-Sized Tire-Derived Aggregate for Embankment Application. *J. Mater. Civ. Eng.* **2013**, *25*, 1285–1290. [[CrossRef](#)]
76. Zahran, K.; El Naggar, H. Effect of Sample Size on TDA Shear Strength Parameters in Direct Shear Tests. *Transp. Res. Rec.* **2020**, *2674*, 1110–1119. [[CrossRef](#)]
77. Cui, X.; Du, B.; Xiao, H.; Zhou, R.; Guo, G.; Liu, H. Interface Damage and Arching Mechanism of CRTS II Slab Track under Temperature Load. *Constr. Build. Mater.* **2021**, *291*, 123258. [[CrossRef](#)]
78. *BS EN 206:2013*; BSI Standards Publication Concrete—Specification, Performance, Production and Conformity. BSI Standards: London, UK, 2013.
79. Cebasek, T.M.; Esen, A.F.; Woodward, P.K.; Laghrouche, O.; Connolly, D.P. Full Scale Laboratory Testing of Ballast and Concrete Slab Tracks under Phased Cyclic Loading. *Transp. Geotech.* **2018**, *17*, 33–40. [[CrossRef](#)]
80. Kramer, S. *Geotechnical Earthquake Engineering*; Prentice Hall: Upper Saddle River, NJ, USA, 1996.
81. McCartney, J.S.; Ghaaowd, I.; Fox, P.J.; Sanders, M.J.; Thielmann, S.S.; Sander, A.C. Shearing Behavior of Tire-Derived Aggregate with Large Particle Size. II: Cyclic Simple Shear. *J. Geotech. Geoenviron. Eng.* **2017**, *143*, 04017078. [[CrossRef](#)]
82. Hall, L. Simulations and Analyses of Train-Induced Ground Vibrations in Finite Element Models. *Soil Dyn. Earthq. Eng.* **2003**, *23*, 403–413. [[CrossRef](#)]
83. Hay, W. *Railroad Engineering*; John Wiley & Sons Inc.: Hoboken, NJ, USA, 1982.